INTERNATIONAL JOURNAL FOR NUMERICAL METHODS IN FLUIDS
Int. J. Numer. Meth. Fluids 2008; **56**:1069–1076
Published online in Wiley InterScience (www.interscience.wiley.com). DOI: 10.1002/fld.1739

High-order methods and mesh adaptation for Euler equations

F. Alauzet*, †

INRIA-Gamma Project, Domaine de Voluceau, Le Chesnay 78153, France

SUMMARY

In this paper, we point out a novel contribution of mesh adaptation to high-order methods for stationary and time-dependent problems. From theoretical results, we exhibit that mesh adaptation, based on an adjoint-free method, achieves a global second-order mesh convergence for numerical solutions with discontinuities in $\mathbf{L}^p$ norm. To attain this result, it is mandatory to combine together all mesh adaptive methods developed in the previous work. This theoretical result is validated on 2D and 3D examples for stationary and time-dependent simulations. Copyright © 2008 John Wiley & Sons, Ltd.

Received 19 April 2007; Revised 28 November 2007; Accepted 5 December 2007

KEY WORDS: anisotropic mesh adaptation; unstructured meshes; high-order method; Euler equations

1. INTRODUCTION

Classical high-order shock capturing methods, such as MUSCL, ENO, residual distribution scheme, etc. are theoretically converging at order two or more. Such methods are suitable to compute discontinuous flows that often occur for supersonic flows, blast waves, interfaces' problems, etc. Nevertheless, this theoretical order is never obtained in practice. Only an order less than one is attained when the mesh is uniformly refined. Indeed, by meshing uniformly a segment, we can demonstrate that in a discontinuity the interpolation error converges in $\mathcal{O}(h^{1/p})$ for $\mathbf{L}^p$ norm. Similarly when sharp gradients are present in the flow field, the theoretical asymptotic order is only reached when the mesh size is sufficiently small.

In the field of computational fluid dynamics (CFD), unstructured mesh adaptation is well known to improve the accuracy of solutions, i.e. it increases the ratio between solution accuracy and the inverse number of degrees of freedom. Thus, enabling substantial gains in CPU, memory requirement and storage space. Visualization of the results is also facilitated. Furthermore, error estimates have the capability to detect physical phenomena and capture their behavior. Meshes are thus automatically adapted in critical regions without any *a priori* knowledge of the problem. Recently,

*Correspondence to: F. Alauzet, INRIA-Gamma Project, Domaine de Voluceau, Le Chesnay 78153, France.
†E-mail: frederic.alauzet@inria.fr

convergence analysis was derived for scalar output in the case of adjoint-based adaptation [1, 2], also called goal-oriented mesh adaptation. However, global convergence of the whole adapted solution is rarely theoretically analyzed nor numerically observed.

The aim of this paper is to focus on one novel contribution of mesh adaptation for high-order shock capturing methods. We point out that mesh adaptation, based on an adjoint-free method, increases the order of convergence in discontinuities. This result implies that the theoretical global second order of mesh convergence of numerical schemes is recovered by means of adaptive techniques in the context of discontinuous flows. All the requirements needed in an attempt to reach this theoretical order are provided in this paper. These requirements are methods developed in previous works [3, 4]. In other words, this paper presents a synthesis of all previous works and shows that combined together they impact the convergence order of numerical methods.

For steady flows, we establish that the theoretical asymptotic order in the $\mathbf{L}^p$ norm is reached for the whole solution field with anisotropic mesh adaptation, even if sharp gradients or discontinuities are present in the flow field. It is based on the continuous metric concept and the convergence of the adapted mesh at a fixed accuracy. The extension to transient problems is proposed but requires more efforts since time accuracy is also involved. To address this issue, we utilize a generalization of the mesh adaptation algorithm for unsteady simulations coupled with a metric intersection in time procedure and a conservative solution transfer.

2. STATIONARY PROBLEMS

The generation of anisotropic adapted meshes uses the notion of length in a metric space [5]. The introduction of a metric tensor in the dot product definition curves the Euclidean space by prescribing sizes and directions. The mesh is automatically adapted by generating *a unit mesh* with respect to this metric, i.e. the mesh is such that all edges have a length close to one in the metric and such that all elements are almost regular. A metric is a $n \times n$ symmetric definite positive matrix, where n is the space dimension. When this metric is continuously defined over the whole domain, it is called a *continuous metric*. For steady flows, achieving the global theoretical order of mesh convergence relies on the continuous metric concept and the convergence of the adapted mesh at a fixed accuracy.

Continuous metric: This concept is based on equivalence classes of meshes [4]. The metric is then seen as the continuous class representative of all meshes having the same global interpolation error level value for a given number of vertices. In the following, we precise how the metric is derived.

Let u be an analytic solution defined on a bounded domain Ω and N be the desired number of vertices for the mesh. We aim at creating the 'best' mesh $\mathscr{H}$, i.e. to find the optimal continuous metric $\mathscr{M}$, that minimizes the interpolation error $(u-\Pi_h u)$ in $\mathbf{L}^p$ norm with N vertices. $\Pi_h u$ denotes the linear interpolate of u on $\mathscr{H}$. To this end, a model of the interpolation error with respect to a metric $\mathscr{M}$, denoted $e_{\mathscr{M}}$, is required.

In [4], a model of the interpolation error for a metric $\mathscr{M}$ is given. It has been proved that locally the optimal metric has for main directions the eigenvectors of the Hessian of u. Let $\mathscr{R}_u$ and Λ be Hessian's eigenvectors and eigenvalues matrices. Then, the local error model for such metric in the neighborhood of a vertex a could be simplified to $e_{\mathscr{M}}(a)=\sum_{i=1}^{n} h_i^2 |\partial^2 u/\partial \alpha_i^2|$, where h_i and $\partial^2 u/\partial \alpha_i^2$ stand for sizes prescribed by the metric and the eigenvalues of the Hessian in the

DOI: 10.1002/fld

direction of the ith eigenvectors of the Hessian, respectively. Now, we are looking for the function $\mathscr{M}$ that minimizes, for a given number N of vertices, the $\mathbf{L}^p$ norm of this error. Therefore, we have to solve the problem:

$$\min_{\mathscr{M}} \mathscr{E}(\mathscr{M}) = \min_{\mathscr{M}} \left(\int_\Omega (e_{\mathscr{M}}(\mathbf{x}))^p \, \mathrm{d}\mathbf{x} \right)^{1/p} = \min_{h_i} \left(\int_\Omega \left(\sum_{i=1}^{n} h_i^2(\mathbf{x}) \left| \frac{\partial^2 u}{\partial \alpha_i^2}(\mathbf{x}) \right| \right)^p \mathrm{d}\mathbf{x} \right)^{1/p} \tag{1}$$

under the constraint:

$$\mathscr{C}(\mathscr{M}) = \int_\Omega \prod_{i=1}^{n} h_i^{-1}(\mathbf{x}) \, \mathrm{d}\mathbf{x} = \int_\Omega \mathrm{d}(\mathbf{x}) \, \mathrm{d}\mathbf{x} = N \tag{2}$$

The resulting optimal metric solution of problem (1)–(2) for the $\mathbf{L}^p$ norm in n-dimensions reads

$$\mathscr{M}_{\mathbf{L}^p} = D_{\mathbf{L}^p} (\det |H_u|)^{-1/(2p+n)} \mathscr{R}_u^{-1} |\Lambda| \mathscr{R}_u \quad \text{with } D_{\mathbf{L}^p} = N^{2/n} \left(\int_\Omega \left| \prod_{i=1}^{n} \frac{\partial^2 u}{\partial \alpha_i^2} \right|^{p/(2p+n)} \right)^{-2/n} \tag{3}$$

$D_{\mathbf{L}^p}$ is a global normalization term to obtain a mesh with N vertices, and $(\det |H_u|)^{-1/(2p+n)}$ is a local normalization term accounting for the sensitivity of the $\mathbf{L}^p$ norm. Indeed, the choice of a $\mathbf{L}^p$ norm is essential in a mesh adaptation process regarding the type of problem solved. For instance in CFD, physical phenomena can involve large-scale variations. Capturing weak phenomena is crucial for obtaining an accurate solution by taking into account all phenomena interactions in the main flow area. Intrinsically, metrics constructed with lower p norms are more sensitive to weaker variations of the solution, whereas the $\mathbf{L}^\infty$ norm mainly concentrates on strong singularities (e.g. shocks).

Mesh convergence order: The expression of the error committed with the optimal metric $\mathscr{M}_{\mathbf{L}^p}$ is deduced from relations (1) and (3):

$$\mathscr{E}(\mathscr{M}_{\mathbf{L}^p}) = n N^{-2/n} \left(\int_\Omega \left| \prod_{i=1}^{n} \frac{\partial^2 u}{\partial \alpha_i^2} \right|^{p/(2p+n)} \right)^{(2p+n)/pn} \leqslant \frac{Cst}{N^{2/n}} \tag{4}$$

Two main results arise from this relation:

- The interpolation error obtained with the resulting metric $\mathscr{E}(\mathscr{M}_{\mathbf{L}^p})$ is optimal in $\mathbf{L}^p$ norm, i.e. a larger error is committed whatever the considered metric prescribing N vertices (see [4] for the proof).
- A global second-order asymptotic mesh convergence is expected for the considered variable u even if singularities are present in the flow field for all p's.

As regards the mesh convergence order, a simple analogy with regular grids leads to consider that $N = O((\prod_{i=1,n} h_i)^{-1}) = O((h^n)^{-1})$ so that the previous estimate becomes $\mathscr{E}(\mathscr{M}_{\mathbf{L}^p}) \leqslant Cst' h^2$. Practically, this result means that in vicinity of discontinuities, the density of nodes prescribed by the mesh adaptation strategy is such that the global second-order mesh convergence holds.

This theoretical order has been demonstrated for a smooth function. However, some difficulties arise when the solution is given by a numerical scheme. Contrary to mesh adaptation for functions, the accuracy level of the solution depends on the current mesh used for its computation. An iterative process needs to be set up in order to converge both the mesh and the solution, or equivalently

DOI: 10.1002/fld

the metric field and the solution. The second issue is that we deal with numerical solutions that are not twice continuously differentiable.

Mesh adaptation scheme: Anisotropic mesh adaptation is a non-linear problem. Therefore, an iterative procedure is required to solve this problem. For stationary simulations, an adaptive computation is carried out via a mesh adaptation loop inside which an algorithmic convergence of the mesh-solution couple is sought. At each stage, a numerical solution is computed on the current mesh with the flow solver and is analyzed with an error estimate. The continuous metric theory described above is considered to estimate the error. As the control is performed on the interpolation error, this approach is independent of the problem at hand. This anisotropic metric is a function of the solution's Hessian which is reconstructed from the numerical solution by a double $\mathbf{L}^2$ projection. Next, an adapted mesh, i.e. a unit mesh, is generated with respect to this metric. Mesh generators use all meshing operations to adapt the mesh and a vertex insertion procedure based on an anisotropic generalization of Delaunay technique. Finally, the solution is linearly interpolated on the new mesh. This procedure is repeated until convergence of the couple mesh-solution.

Application to numerical computation: In our case, the numerical solution provides a continuous piecewise linear by element representation of the solution. Consequently, our analysis cannot be applied directly to the numerical solution. The idea is to build a higher-order solution approximation u^* of u from u_h which is twice continuously differentiable and to consider u^* in our error estimate. More precisely, the approximation error could be approximated as $\|u-u_h\|_{p,\Omega} \approx \|u^*-u_h\|_{p,\Omega}$. The Hessian of u^* is recovered by a double L^2 projection algorithm.

In the context of discontinuous flows, the numerical solution is also piecewise linear by elements even if it approximates a discontinuous solution. The mesh acts as a convolution operator on the solution. In this case, we still approximate the solution u with a continuous higher-order representation and we still apply our error estimate.

3. TIME-DEPENDENT PROBLEMS

The extension to time-dependent problem requires more effort since time accuracy is involved. Indeed, the continuous metric concept does not take into account time accuracy. For explicit discretization in time, one can show with a truncature analysis that the error in space control the error in time under Courant–Friedrichs–Lewy condition. Consequently, to control the solution accuracy we have to control the error in space throughout a given time frame of computation. To address this issue, we have proposed a generalization of the mesh adaptation algorithm for unsteady simulations coupled with metric intersection in time [3]. Then, to reduce the error due to the interpolation stage, a conservative solution transfer is considered.

Transient fixed-point mesh adaptation scheme: To solve the non-linear problem of mesh adaptation for unsteady simulation, a novel algorithm generalizing the mesh adaptation scheme has been proposed in [3]. This procedure, based on the resolution of a transient fixed point problem for the couple mesh-solution at each iteration of the mesh adaptation loop, predicts the solution evolution in the computational domain. Knowing then the solution evolution throughout a short period of time, the mesh is suitably adapted in all regions where the solution progresses so as to preserve its accuracy. To this end, a metric intersection in time procedure is introduced in the metric construction, thereby the time variable is implicitly introduced in the error estimate. Consequently, this scheme controls the spatial and the time error throughout the computation.

DOI: 10.1002/fld

Conservative interpolation: After generating a new mesh, the solution is transferred or interpolated from the previous mesh to this new adapted mesh. This stage becomes crucial in the context of unsteady problems. Actually, for second-order methods for conservation laws this stage must be P^1-exact and conservative. In this aim, a solution transfer process based on mesh intersection has been proposed. For each element of the new mesh, we compute and mesh (with simplices) the geometric intersection with each element of the previous mesh that it overlaps. Thus, we are able to compute the mass using Gauss quadrature formula and the gradient on each simplex of the new mesh. Finally, nodal value solution is reconstructed from this piecewise by element discontinuous representation.

Conclusion: The space–time mesh obtained produces an optimal convergence order. The convergence cannot be second order for the space–time mesh since the time step (discretization) $\mathrm{d}t_n$ is spatially uniform at each time level n. However, as the transient fixed-point mesh adaptation scheme controls the error in space and in time, the theory predicts a second-order spatial mesh convergence for the numerical solution at a given instant t.

4. NUMERICAL RESULTS

The predicted theoretical mesh convergence order is numerically assessed on 2D and 3D internal and external simulations. In all examples, the flow is modeled by the conservative Euler equations. Assuming that the gas is perfect, these equations could be symbolically rewritten as $\partial W/\partial t + \nabla \cdot F(W) = 0$, where $W = {}^t(\rho, \rho u, \rho v, \rho w, \rho E)$ is the conservative variables vector and the vector F represents the convective operator. We have denoted by ρ the density, $\mathbf{U} = (u, v, w)$ the velocity vector and E the total energy.

The Euler system is solved with a finite volume technique on unstructured triangular or tetrahedral meshes. The proposed scheme is second-order accurate in space and time. This scheme is vertex centered and uses a particular edge-based formulation with upwind elements [6]. The flow solver utilizes a HLLC approximate Riemann solver to compute numerical fluxes. High-order scheme is derived according to a MUSCL-type method using downstream and upstream simplex combined with a generalization of the Superbee limiter with three entries to guarantee the TVD property of the scheme [7]. An explicit time stepping algorithm is used by means of a five-stage, second-order strong-stability-preserving Runge–Kutta scheme.

For each computation, we set for each type of mesh the reference solution as the solution obtained on the finest mesh of this type. In other words, the reference solution for uniform (resp. adapted) meshes computations is the solution on the finest uniform (resp. adapted) mesh. Then, the error is calculated by comparing the computed solution with the reference one on the finest mesh. More precisely, the computed solution is transferred on the associated reference mesh. Thereafter, the error is evaluated on the reference mesh using quadrature rule.

Scramjet internal flow: The scramjet configuration at Mach 3 is typical of numerical simulations in compressible fluids involving highly anisotropic phenomena with very strong shocks. We control the $\mathbf{L}^1$ norm or $\mathbf{L}^2$ norm of the error on the pressure for adaptations. The final adapted mesh in $\mathbf{L}^1$ norm containing 22 566 vertices and the corresponding density isolines are shown in Figure 1. The same figure (right) reports pressure errors in $\mathbf{L}^1$ and $\mathbf{L}^2$ norms for computations performed on uniform and adapted meshes. A first and a second-order mesh convergence is obtained for the uniform and adapted cases, respectively. We obtain the same orders of convergence for the density and the Mach number even if we adapt only on the pressure.

DOI: 10.1002/fld

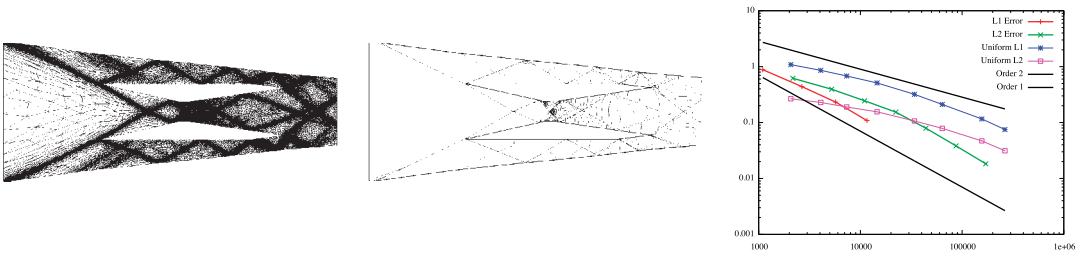

Figure 1. Scramjet simulation. Final anisotropic mesh with $\mathbf{L}^1$ norm continuous metric-based adaptation (left) and the associated density isolines (middle). Right: mesh convergence order in $\mathbf{L}^1$ and $\mathbf{L}^2$ norms for the pressure.

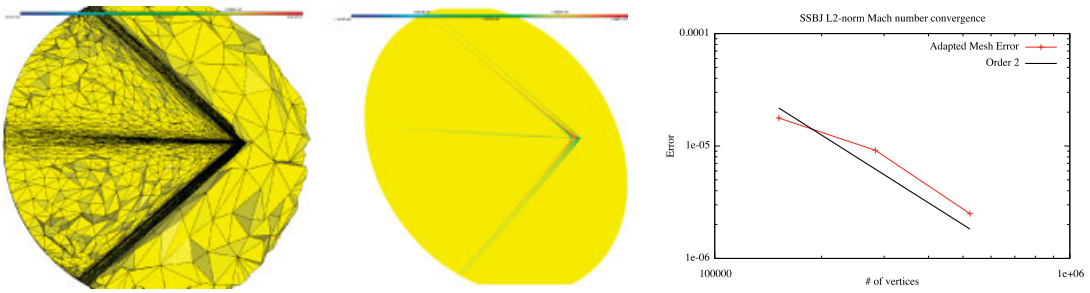

Figure 2. The 3D supersonic aircraft simulation. Left: final anisotropic mesh with $\mathbf{L}^2$ norm adaptation. Middle: final Mach number iso-value in the symmetry plane. Right: order of mesh convergence in $\mathbf{L}^2$ norm for the Mach number.

Supersonic aircraft: This 3D supersonic case involves an aircraft's complex geometry included in a 1 km spherical domain. The aircraft is flying at Mach 1.6 with an angle of attack of 3°. We control the $\mathbf{L}^2$ norm of the error on the Mach number, as it is really a representative of external flows. Refinement and shock waves have been propagated in the whole computational domain, Figure 2, with a final anisotropic adapted mesh containing 569 161 vertices (almost 3.3 millions tetrahedra). For this 3D stationary case, second-order convergence has been attained for the Mach number.

Four shocks Riemann problem: This time-dependent problem is a 2D Riemann problem. Initially, four constant states are set in each quarter of the square domain such that four shock waves propagate [8]. The mesh is adapted on the density controlling the $\mathbf{L}^1$ norm or $\mathbf{L}^2$ norm of the error. The final density and the related adapted mesh in $\mathbf{L}^1$ norm at a dimensional time $t = 0.25$ are presented in Figure 3. Density spatial mesh convergence order is analyzed on uniform and adapted meshes for the final solution. As expected, a second order is reached for the adapted approach whereas we obtain only first order for uniform meshes. We obtain the same orders of convergence for the pressure and the Mach number even if we adapt only on the density.

3D blast in a town: Finally, a 3D blast wave simulation in a city plaza is presented to emphasize the applicability of the proposed approach for realistic problems. No convergence analysis has been performed due to the complexity of the problem. In this case, the mesh has been adapted

DOI: 10.1002/fld

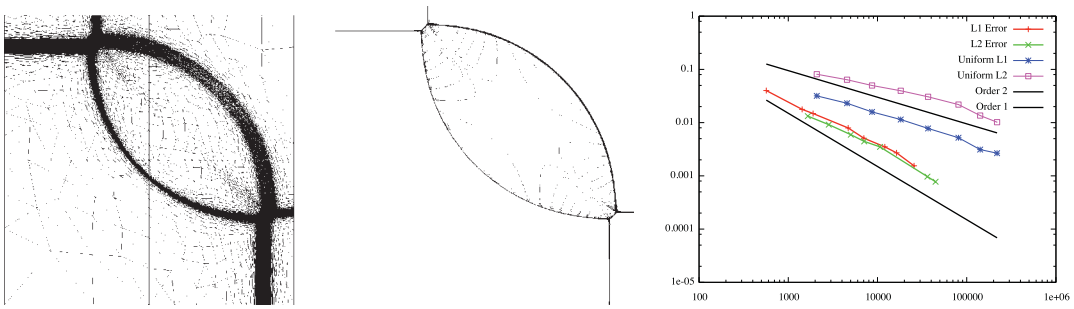

Figure 3. Four shocks Riemann problem simulation. Final anisotropic mesh with $\mathbf{L}^2$ norm continuous metric-based adaptation (left) and the associated density isolines (middle). Right: mesh convergence order in $\mathbf{L}^1$ and $\mathbf{L}^2$ norms for the density.

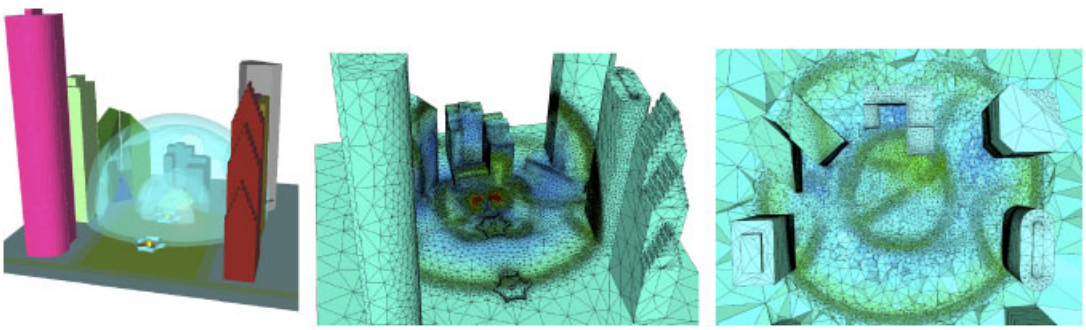

Figure 4. 3D blast in a town simulation. Left: progression of the density's iso-surfaces. Middle, isotropic adapted surface mesh. Right: top view of the isotropic adapted volume mesh in a cut parallel to the ground.

isotropically in $\mathbf{L}^\infty$ norm on the density variable. A perturbation, corresponding to the initial conditions of the Sod's shock tube problem [9] is introduced into a uniform field so as to simulate an explosion in the city. Snapshots of the solution and the associated adapted surface and volume meshes (containing almost 4.3 millions tetrahedra) are shown in Figure 4.

REFERENCES

1. Giles MB, Pierce NA. In *Adjoint Error Correction for Integral Outputs*. Lecture Notes in Computational Science and Engineering, vol. 25, Barth T, Deconinck H (eds). Springer: Berlin, 2002; 47–96.
2. Venditti D, Darmofal D. Grid adaptation for functional outputs: application to two-dimensional inviscid flows. *Journal of Computational Physics* 2002; **176**(1):40–69.
3. Alauzet F, Frey PJ, George P-L, Mohammadi B. 3D transient fixed point mesh adaptation for time-dependent problems: application to CFD simulations. *Journal of Computational Physics* 2007; **222**:592–623.
4. Alauzet F, Loseille A, Dervieux A, Frey PJ. Multi-dimensional continuous metric for mesh adaptation. *Proceedings of 15th International Meshing Rountable*. Springer: Berlin, 2006; 191–214.
5. Frey PJ, George P-L. *Mesh Generation. Application to Finite Elements*. Hermès Science: Paris, Oxford, 2000.
6. Debiez C, Dervieux A. Mixed-element-volume MUSCL methods with weak viscosity for steady and unsteady flow calculations. *Computers and Fluids* 2000; **29**:89–118.

DOI: 10.1002/fld

7. Cournède P-H, Koobus B, Dervieux A. Positivity statements for a mixed-element-volume scheme on fixed and moving grids. *European Journal of Computational Mechanics* 2006; **15**(7–8):767–798.
8. Schulz-Rinne CW, Collins JP, Glaz HM. Numerical solution of the Riemann problem for two-dimensional gas dynamics. *SIAM Journal on Scientific Computing* 1993; **14**(6):1394–1414.
9. Sod GA. A survey of several finite difference methods for systems of nonlinear hyperbolic conservation laws. *Journal of Computational Physics* 1978; **27**:1–31.

DOI: 10.1002/fld